



Temporal Inhomogeneities in High-Resolution Gridded Precipitation Products for the Southeastern United States

- 3 Jeremy E. Diem¹
- 4 Department of Geosciences, Georgia State University, Atlanta, GA, 30303, USA
- 5 Correspondence to: Jeremy E. Diem (jdiem@gsu.edu)
- Abstract. High-resolution gridded precipitation products are widely used in hydroclimatic analyses, although their long-term 6 stability has not been thoroughly evaluated. This study investigates temporal inhomogeneities in five widely used 7 precipitation datasets—Daymet, gridMET, nClimGrid, PRISM, and TerraClimate—across the southeastern United States 8 9 during 1980-2024. Annual precipitation totals were derived from both monthly and daily data and compared with a 10 reference time series constructed from 120 U.S. Cooperative Observer Program (COOP) gauges. Residual-mass curves and 11 Mann-Whitney U tests were applied to identify temporal inhomogeneities, and trend magnitudes were estimated using the 12 Kendall-Theil robust line. Significant inhomogeneities were detected in most datasets, with nearly 80% of discontinuities concentrated between 2002 and 2018. These shifts corresponded closely to changes in gauge-network composition and data-13 processing procedures. Daymet and PRISM exhibited wetting biases linked to the expansion of the Community 14 Collaborative Rain, Hail, and Snow (CoCoRaHS) network and the concurrent decline of COOP gauges, whereas nClimGrid 15 16 showed a drying bias resulting from increased reliance on Automated Surface Observing System tipping-bucket gauges, 17 which underestimate rainfall. Step increases in TerraClimate and gridMET totals reflected transitions in input data and reprocessing of precipitation forcing fields. These inhomogeneities produced disparate multi-decadal trends ranging from 19 18 19 to 48 mm dec⁻¹ compared with a non-significant reference trend of 30 mm dec⁻¹. Among all datasets and combinations 20 tested, the Daymet-nClimGrid pair was the only one without detectable discontinuities and reproduced the reference trend 21 most accurately. This combination provides a homogeneous, temporally consistent dataset for multi-decadal precipitation 22 analyses across the Southeast. Overall, the results demonstrate that unrecognized inhomogeneities in gridded precipitation products can substantially bias regional trend assessments and underscore the need to evaluate and, when necessary, combine 23 24 datasets to ensure temporal stability in long-term hydroclimatic studies.

25 1 Introduction

- 26 High-quality, multi-decadal precipitation data are essential for research and decision-making. Such records enable rigorous
- 27 assessment of variability and long-term trends (New et al., 2001) and provide a robust foundation for model calibration and
- 28 evaluation (Döll et al., 2016; Tango et al., 2025). Reliable long-term observations also underpin integrated and adaptive



31

33

40

41

42

43 44

45

46 47

48

49

50

51

52

53



29 management of water resources, supporting sustainable planning for agriculture, ecosystems, and regional development

30 (Yang et al., 2021; Ferencz et al., 2024;).

Spatial limitations remain a persistent challenge in precipitation measurement. Although gauge networks provide the 32 foundation for precipitation observation, gauge distribution is often sparse and uneven (Kidd et al., 2017). These deficiencies are most pronounced in complex terrain and other data-sparse regions (Michelon et al., 2021).

34 To extend coverage beyond existing gauges, gridded precipitation products were developed. These datasets integrate gauge, 35 satellite, and reanalysis information through interpolation or merging algorithms to generate spatially continuous 36 precipitation estimates (Mankin et al., 2025). Gauge-informed products generally provide higher spatial accuracy than those derived solely from remote sensing or reanalysis (Zandler et al., 2019; Muche et al., 2020; de la Fraga et al., 2024; Mankin et 37 38 al., 2025). However, the limited availability of gauges in complex terrain still constrains accuracy, and many products 39 perform poorly in mountainous regions (Zandler et al., 2019; de la Fraga et al., 2024; Wang and Tian, 2025).

High-resolution gridded precipitation products are particularly well-suited to the needs of the hydrology community, which relies on them more than any other discipline. Gridded precipitation datasets provide the spatially distributed input data required to drive hydrologic models (Livneh et al., 2015; Newman et al., 2015; Shuai et al., 2022). Among many other applications, gridded precipitation products are also employed to quantify basin-scale water balances (Laiti et al., 2018) and to support hydrologic forecasting and management (Mankin et al., 2025).

Despite the widespread use of gridded precipitation products, especially within the hydrology community, the temporal stability of these datasets remains insufficiently evaluated. Apparent long-term trends can be distorted by inhomogeneities systematic, non-climatic shifts in the statistical properties of a time series (Peterson et al., 1998). Only a handful of studies (e.g., Guentchev et al., 2010; Mizukami and Smith, 2012; McAfee et al., 2014; Ferguson and Mocko, 2017; Henn et al., 2018) have explicitly identified or investigated such inhomogeneities in gridded precipitation products. Accordingly, this study evaluates the temporal stability of multiple high-resolution precipitation datasets across a large, climatically uniform region during 1980-2024. The objectives are to (1) detect and characterize temporal inhomogeneities and the factors contributing to them, (2) quantify biases that influence multi-decadal trends, and (3) determine which individual products or product combinations exhibit the greatest temporal stability for regional trend analyses.

This study focuses on the southeastern United States (Fig. 1), encompassing Alabama, Florida, Georgia, Mississippi, 54 55 North Carolina, South Carolina, and Tennessee, with a total area of approximately 882,000 km². The Southeast was selected because much of it has a humid subtropical climate—hot summers, mild winters, and high annual precipitation (Kunkel et 56 al., 2013; Labosier and Quiring, 2013)—and includes numerous long-term reference gauges from the U.S. Cooperative 57 58 Observer Program (COOP), the nation's most consistent climate network (National Research Council, 1998).





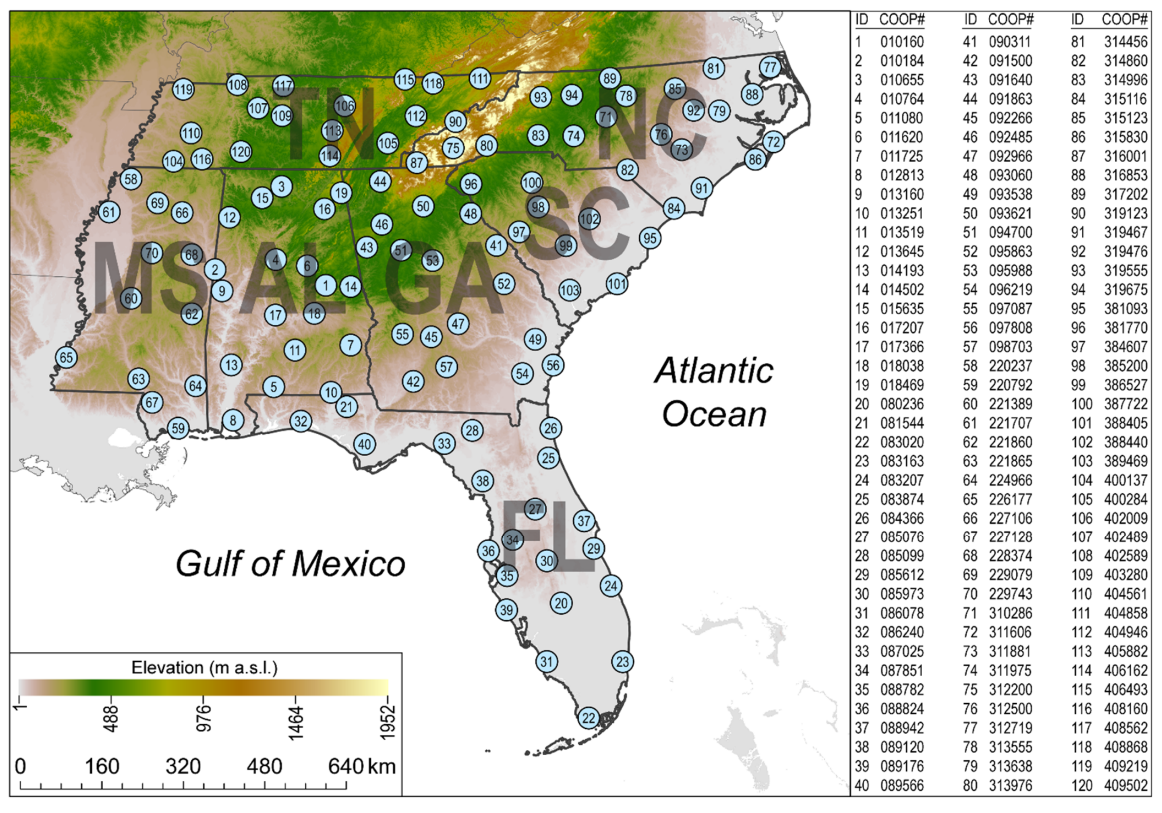


Figure 1. Locations of the 120 reference gauges in the southeastern United States. All gauges are part of the U.S. Cooperative (USC) network. The seven states that comprise the southeastern United States are Alabama (AL), Florida (FL), Georgia (GA), Mississippi (MS), North Carolina (NC), South Carolina (SC), and Tennessee (TN).

2 Data

59 60

62

63

70

71

72

Monthly precipitation totals from a dispersed network of 120 COOP gauges across the Southeast during 1980-2024 were used to produce a reference time series (Fig. 1). All gauges had at least 90% of months with precipitation totals. Only 1.6% of gauge-months were missing. The missing monthly totals were replaced with the mean total from the three closest gauges. The gauges ranged in elevation from 1 m a.sl. to 668 m a.sl.; therefore, none of the gauges were located in high-elevation areas. Monthly totals for each gauge were summed to produce annual precipitation values, which were then averaged across all gauges to form the regional reference time series.

Precipitation estimates were obtained for five high-resolution gridded products (Daymet, gridMET, nClimGrid, PRISM, and TerraClimate) for 1980–2024. For each product, annual precipitation totals were derived from the available daily and monthly data. Daymet provides daily precipitation estimates for North America at 1-km resolution, with monthly values





73 derived by aggregating daily fields (Thornton et al., 2021). Daymet data were not yet released for 2024 at the time of 74 analysis; therefore, the Daymet series extends through 2023. nClimGrid provides daily and monthly precipitation estimates 75 for the conterminous United States at ~4-km resolution, generated independently using climatologically aided interpolation 76 of station data (Vose et al., 2014). PRISM provides daily and monthly precipitation estimates for the United States at ~4-km 77 resolution, generated using station observations integrated with topographic and other spatial predictors (Daly et al., 2008). 78 Because daily PRISM data were not available for 1980, annual totals for that year in the series were derived from monthly 79 PRISM precipitation estimates to maintain a complete 1980-2024 record. gridMET provides daily precipitation estimates for 80 the conterminous United States at ~4-km resolution, generated by combining high-resolution PRISM climatologies with 81 temporally varying fields from the North American Land Data Assimilation System (NLDAS-2) using the METDATA 82 downscaling method (Abatzoglou, 2013). TerraClimate provides monthly precipitation estimates for the global land surface 83 at ~4-km resolution, generated by combining WorldClim climatologies with time-varying anomalies derived primarily from the Climatic Research Unit Time Series (CRU TS) and Japanese 55-year Reanalysis (JRA-55) datasets (Abatzoglou et al., 84 85 2018). When calculating regional means, approximately 2.5 % of grid cells (those exceeding 668 m a.s.l.) were excluded to 86 restrict the analysis to the low- and mid-elevation portions of the Southeast and to minimize the aforementioned precipitation 87 inaccuracies associated with mountainous areas. 88 Information on precipitation gauges underlying each gridded product was compiled for 1980-2024. Gauges were

classified by network, and spatial coverage was assessed by identifying the 40-km grid cell containing each gauge across the Southeast. For each network, the number of grid cells containing at least one gauge was tallied and divided by the total number of grid cells in the region to calculate percent coverage.

In addition to analyzing each gridded product individually, time series were generated for all possible pairwise and

multi-product combinations. Combinations were produced separately for the daily and monthly datasets, with each series calculated as the mean of the contributing products (e.g., Daymet and nClimGrid). For the four products available at both temporal scales, this yielded six two-product combinations, four three-product combinations, and one four-product combination, for a total of 11 unique combinations.

97 3 Methods

89

90

91

92

93

94

95

96

98 3.1 Residual-Mass Curves

Residual-mass curves were constructed as a diagnostic of the homogeneity of precipitation time series and combinations of those series. This approach originates from hydrological consistency testing, in which cumulative residuals are plotted over time to reveal systematic deviations (Searcy and Hardison, 1960). In this study, residuals were obtained from linear regressions in which the reference time series served as the predictor and the product time series as the predictand. For a homogeneous record, the cumulative residuals are expected to remain near zero, fluctuating randomly without systematic





- 104 drift, whereas sustained deviations or changes in slope indicate shifts, biases, or other inconsistencies (Buishand, 1984;
- 105 Helsel and Hirsch, 2002).

106 3.2 Testing for Differences

- 107 To identify the most significant discontinuity—defined here as an abrupt, non-climatic shift in a time series representing a
- 108 temporal inhomogeneity—in each product time series, a nonparametric split-sample approach was applied. For each
- 109 potential breakpoint year, residuals (i.e., observations minus product estimates) before and after that year were compared
- 110 using the Mann-Whitney U test ($\alpha = 0.01$, two-tailed), with a minimum of eight years required in each group, yielding
- 111 candidate breakpoints between 1988 and 2017. The Mann–Whitney U test has been shown to be effective for identifying
- 112 shifts in hydroclimatic time series (Yue and Wang, 2002), and similar split-sample approaches have been applied in climate
- 113 homogenization studies to test for differences before and after potential discontinuities (Easterling and Peterson, 1995).

114 3.3 Trend Analyses

- 115 Trends in annual precipitation for 1980-2024 were computed for each gridded product and the reference time series. The
- 116 Kendall-Theil robust line, calculated as the median of the slopes between all pairs of observations (Helsel and Hirsch, 2002),
- 117 provided a nonparametric estimate of the trend magnitude. The statistical significance of each trend was assessed with
- 118 Kendall's tau correlation test ($\alpha = 0.01$, one-tailed).

119 4 Results

120 4.1 Spatial Variations in Precipitation

- 121 Mean annual precipitation patterns and totals are broadly consistent among the five precipitation products, with Daymet
- 122 producing slightly higher values than the others (Fig. 2). This comparison provides spatial context for the subsequent
- 123 temporal analyses by illustrating that the datasets yield similar climatological means across the Southeast. Mean annual
- 124 totals for 1980–2023 range from 1,347 mm for nClimGrid to 1,431 mm for Daymet. Precipitation totals are smallest (~1,100
- 125 mm) across central Georgia, South Carolina, and North Carolina and largest (~2,000 mm) in the Blue Ridge and Cumberland
- 126 Mountains.

127 **4.2** Changes in Gauges

- 128 All products showed substantial temporal changes in gauge numbers across 1980-2024, most notably increasing coverage by
- 129 CoCoRaHS (Community Collaborative Rain, Hail, and Snow Network) gauges and decreasing coverage by COOP gauges
- 130 (Fig. 3). Daymet was initially dominated by COOP gauges but by the end of the period CoCoRaHS gauges were most
- 131 prevalent. Both CoCoRaHS and weather-bureau gauges increased in coverage, with CoCoRaHS rising from <1% in 2006 to





133

134

135136

137

138139

140

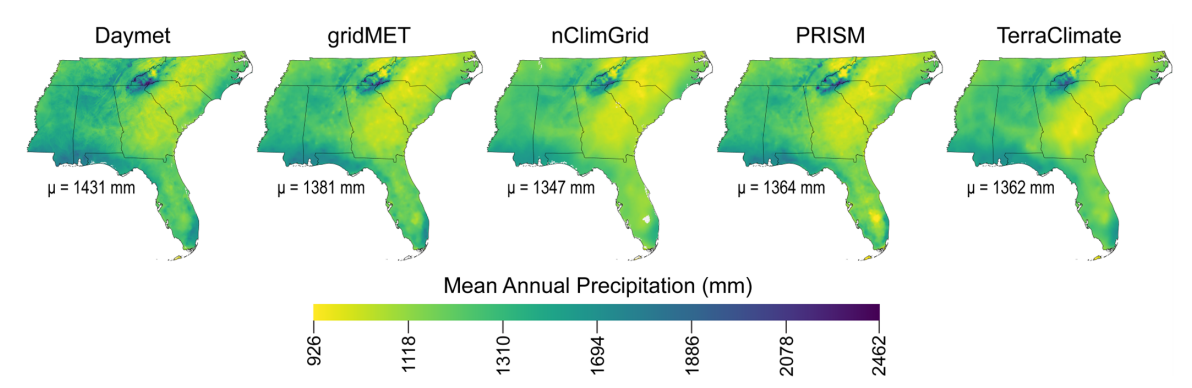


Figure 2. Mean annual precipitation totals (in mm) during 1980-2023 for the five precipitation products. gridMET, nClimGrid, PRISM, and TerraClimate have been resampled to 1-km resolution to match the resolution of Daymet.

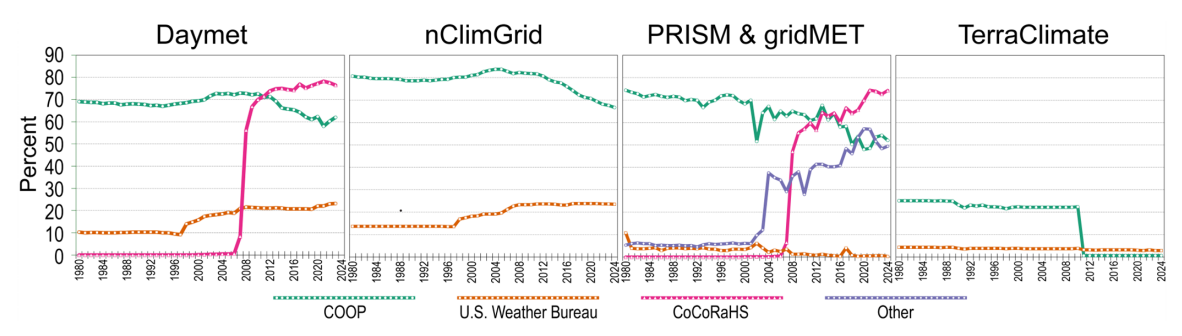


Figure 3. Differences in annual precipitation between monthly products and daily products.

78% in 2021, while COOP gauges began decreasing around 2011. nClimGrid consistently relied more on COOP than weather-bureau gauges, but the difference in 2024 (67% vs. 24%) was much smaller than in 1980 (81% vs. 14%). Coverage by weather-bureau gauges began increasing in 1998, while COOP coverage declined after 2012. PRISM, which used gauges from 15 networks, showed a similar pattern, with increasing CoCoRaHS and decreasing COOP coverage. CoCoRaHS coverage rose from <1% in 2006 to ~75% in 2021. There was also an increase in gauges from other networks and a steady decline in COOP coverage. TerraClimate had much less gauge coverage overall, with a maximum of 25% from cooperative gauges and an abrupt decline from 22% to <1% between 2010 and 2011. Information on gauge coverage for gridMET was unavailable.

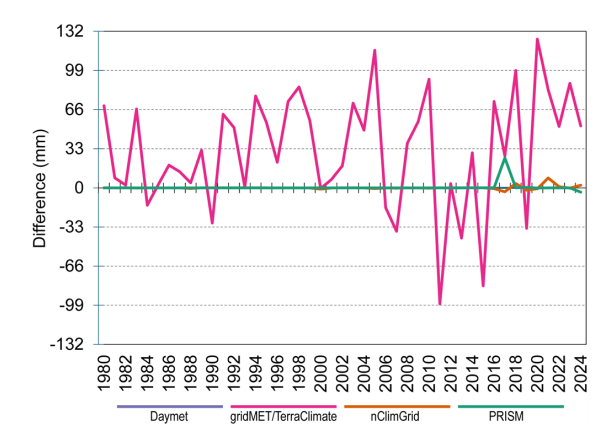
4.3 Comparison of Monthly and Daily Versions of Products

Monthly and daily versions of Daymet, nClimGrid, and PRISM had either identical or nearly identical results (Fig. 4).

Consequently, monthly results—which include TerraClimate—are shown in the paper, while the daily results—which include gridMET—are presented in the supporting information.







145 Figure 4. Percent coverage of the southeastern United States over time by gauge networks used in the five precipitation products.

4.4 Residual-Mass Curves

Among the initial products, Daymet had the most optimal residual-mass curve, and combining products resulted in the best residual-mass curves (Fig. 5 and S1). The best residual-mass curves are those with relatively small cumulative sums of the absolute values of residuals. Daymet had much lower cumulative sums than the other four initial products. The overall best products were combinations of products, and those products were nClimGrid-PRISM, Daymet-nClimGrid-TerraClimate, Daymet-nClimGrid-PRISM, Daymet-gridMET-nClimgrid, and Daymet-nClimGrid.

The residual-mass curves also revealed potential discontinuities, most of which occurred during the third and fourth decades of the 45-year record (Fig. 3 and S2). In each panel of the figures, the year associated with the largest absolute residual corresponded to the year preceding the potential discontinuity. For Daymet, gridMET, nClimGrid, PRISM, and TerraClimate, the potential discontinuities were centered on 2008, 2016, 2005, 2002, and 2011, respectively. For all products and combinations of products, over 80% of the potential discontinuities occurred during 2002-2016.

4.5 Discontinuities

Most products exhibited significant discontinuities, and the timing of these shifts generally aligned with the potential discontinuities identified from the residual-mass curves (Fig. 6 and S2). Approximately 80 % of products showed at least one significant discontinuity. The initial products—Daymet, gridMET, nClimGrid, PRISM, and TerraClimate—had discontinuities centered on 2012, 2016, 2005, 2002, and 2011, respectively. Nearly 90 % of all discontinuities, including those from product combinations, occurred between 2002 and 2018. A few products showed discontinuities in the early 1990s, all of which included nClimGrid as a component. Ideally, no discontinuities should be present in homogeneous time series, and the only products without detectable discontinuities were TerraClimate, Daymet–nClimGrid, nClimGrid–PRISM, and nClimGrid–PRISM—TerraClimate.





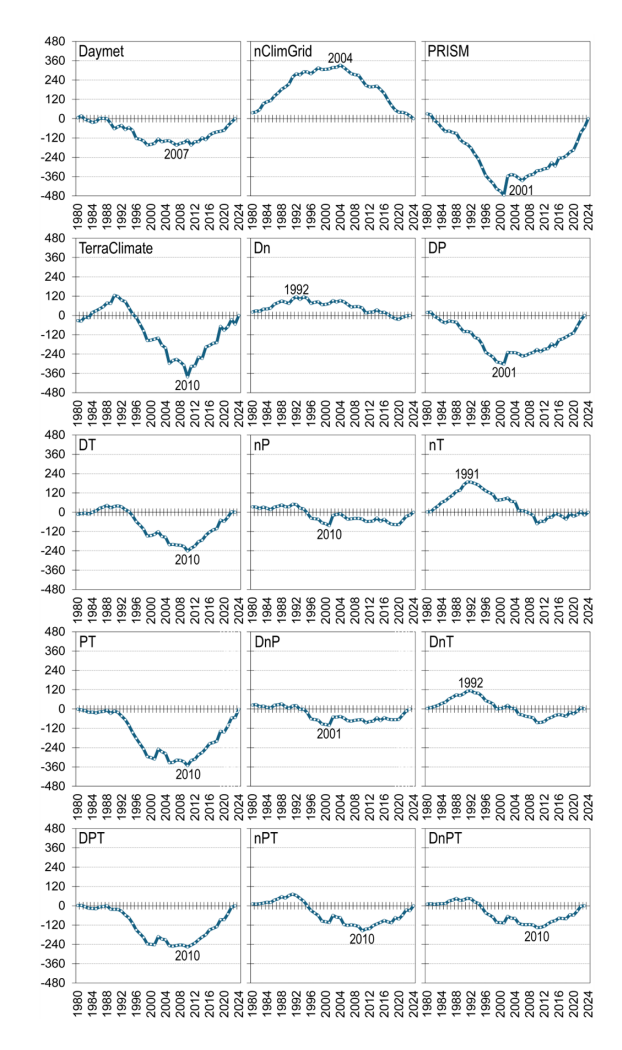


Figure 5. Residual-mass curves for products and combination of products. Abbreviations for Daymet, nClimGrid, PRISM, and
 TerraClimate, are D, n, P, and T, respectively.

4.6 Time Series of Differences

166

169

170

171172

173

With respect to differences from the reference time series before and after a discontinuity, most products shifted from either underestimates to overestimates or from overestimates to larger overestimates (Fig. 7 and S3). Both gridMET and PRISM shifted from underestimates to overestimates. Daymet shifted from overestimates to larger overestimates. nClimGrid shifted from underestimates to larger underestimates. TerraClimate did not exhibit a significant discontinuity and therefore showed no shift. Considering all products collectively, about half shifted from underestimates to overestimates, one-third from





overestimates to larger overestimates, and roughly 17 % from underestimates to larger underestimates; none shifted from overestimates to underestimates.

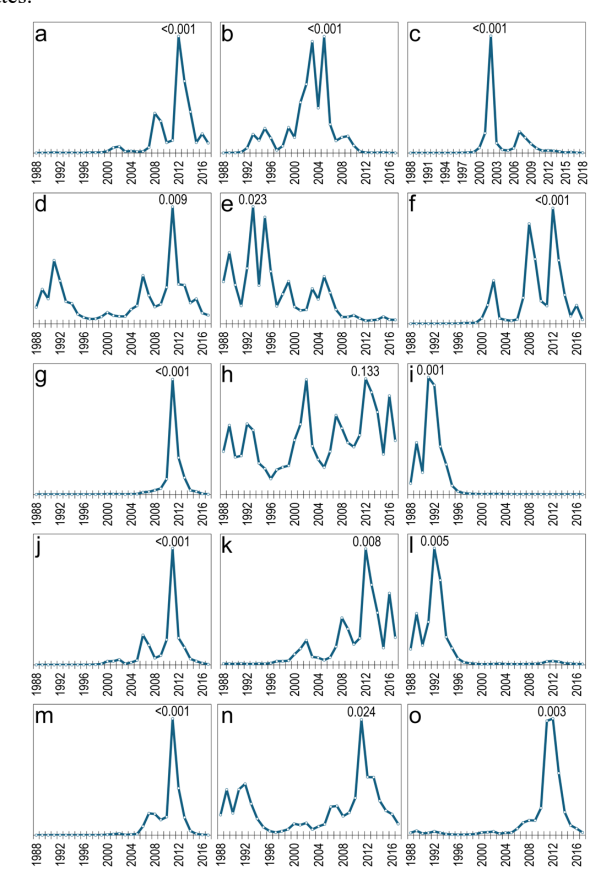


Figure 6. Inverse p-values for (a) Daymet, (b) nClimGrid, (c) PRISM, (d) TerraClimate, (e) Dn, (f) DP, (g) DT, (h) nP, (i) nT, (j) PT, (k) DnP, (l) DnT, (m) DPT, (n) nPT, and (o) DnPT. Abbreviations for Daymet, nClimGrid, PRISM, and TerraClimate, are D, n, P, and T, respectively. The two-tailed p-values are from Mann-Whitney *U* tests that compared differences from the reference time series before and after each of the years shown (i.e., 1988-2018).

4.7 Trends

177

182

The products exhibited a wide range of precipitation trends, with only a few approximating the reference trend of 30 mm dec⁻¹, which was not significant (Fig. 8 and S4). Daymet, gridMET, nClimGrid, PRISM, and TerraClimate had trends of 38, 38, 19, 48, and 36 mm dec⁻¹, respectively. Among the individual products, nClimGrid produced the smallest trend and PRISM the largest trend. The trend for PRISM, as well as those for the combinations Daymet–PRISM, Daymet–gridMET–PRISM, Daymet–PRISM—TerraClimate, gridMET–PRISM, and PRISM—TerraClimate, were statistically significant. The



192

193



products within 10 % of the reference trend were Daymet–gridMET–nClimGrid, Daymet–nClimGrid, gridMET–nClimGrid–189 PRISM, and nClimGrid–TerraClimate.

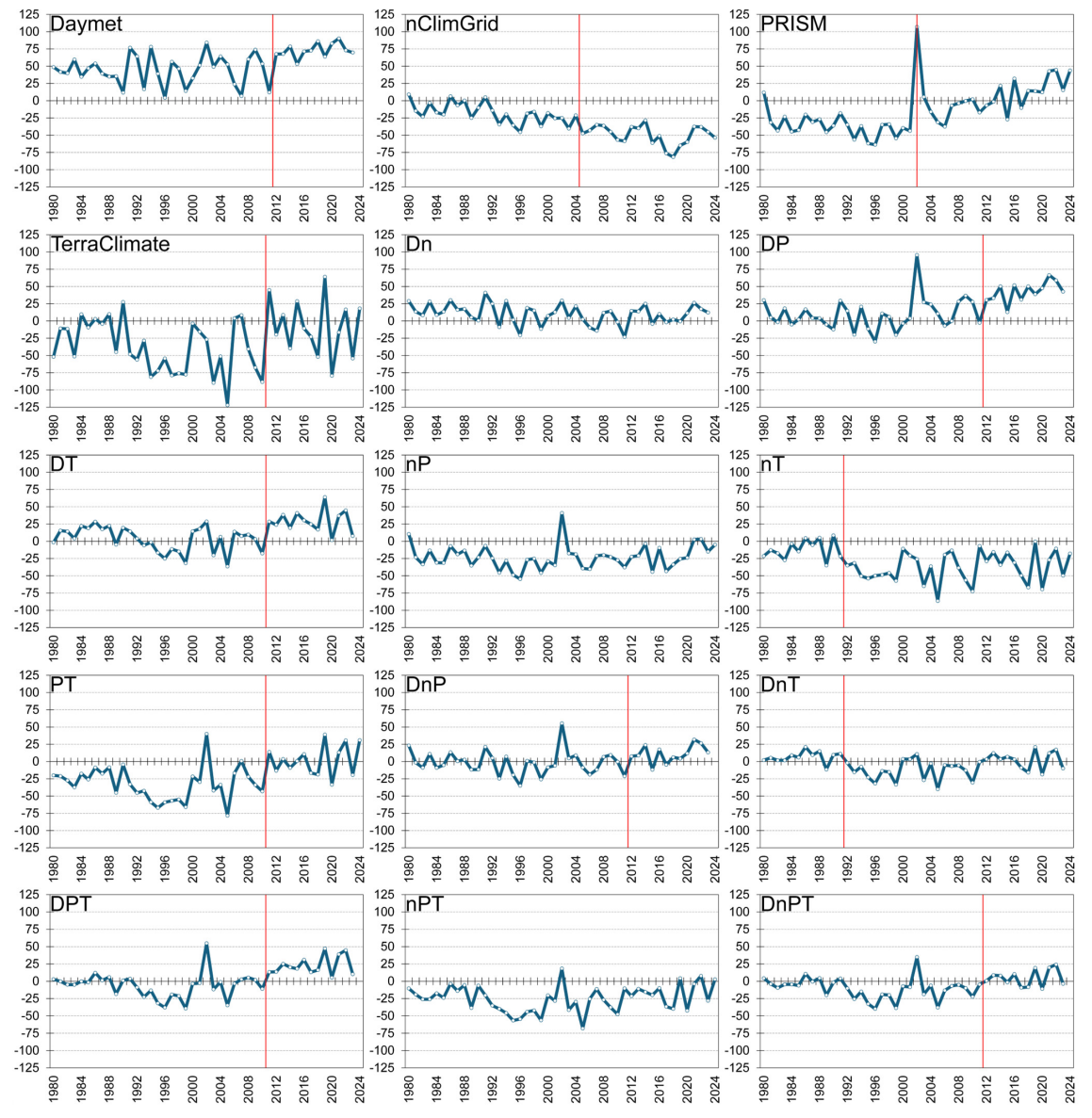


Figure 7. Time series of differences between the mean of the 120 references gauges and the means for the southeastern United States that area specific to products and combination of products. Abbreviations for Daymet, nClimGrid, PRISM, and TerraClimate, are D, n, P, and T, respectively.





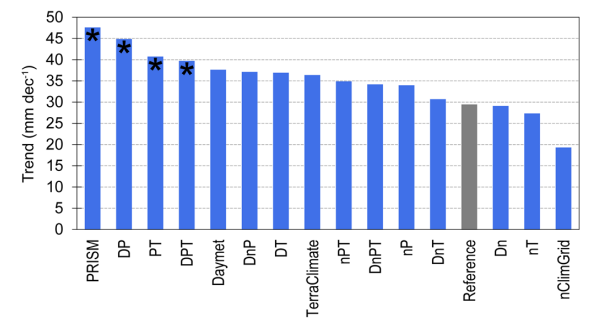


Figure 8. Precipitation increases per decade (in mm) for the reference and 15 other time series. Abbreviations for Daymet, nClimGrid, PRISM, and TerraClimate, are D, n, P, and T, respectively. Asterisks denote significant ($\alpha = 0.01$, one-tailed) trends.

5 Discussion

5.1 Inhomogeneities and Biased Trends of Products

The introduction and proliferation of CoCoRaHS gauges—and to a lesser degree the decline of COOP gauges—caused a wetting bias in the Daymet and PRISM time series. Decadal precipitation increases were 28% and 62% larger, respectively, than those from the reference gauges (Fig. 6). CoCoRaHS gauges generally record slightly higher precipitation totals than COOP gauges, with increases of about 1–5% (CoCoRaHS, 2019; Goble et al., 2019). CoCoRaHS coverage in the Southeast was negligible in 2006 but reached about 75% by 2021, surpassing all other networks by 2012 and 2014 for Daymet and PRISM, respectively (Fig. 2). The largest inhomogeneity in the Daymet series occurred in 2012, coinciding with this expansion. Although PRISM experienced similar network shifts, its main inhomogeneity appeared in 2002 due to anomalously high precipitation; correcting those values shifts the discontinuity to 2007, aligning with the network transition. Expansion of ASOS (Automated Surface Observing Systems) gauges, along with the decline of COOP gauges,

Expansion of ASOS (Automated Surface Observing Systems) gauges, along with the decline of COOP gauges, produced a drying bias in nClimGrid. The decadal precipitation increase for nClimGrid was 34% smaller than that of the reference series (Fig. 6). ASOS instruments use heated tipping-bucket gauges in which each tip represents 0.01 inch of liquid-equivalent precipitation (Wade, 2003). These gauges underestimate rainfall (Dunn et al., 2025), with undercatch of 2–10% relative to COOP observations (National Research Council, 2012). ASOS coverage rose from <1% in 1993 to 19% in 2021 (Fig. 9), while COOP coverage declined from 80% to 70% (Fig. 2). The largest inhomogeneity in nClimGrid occurred in 2005, coinciding with growing ASOS influence.

Abrupt increases in TerraClimate precipitation totals in 2011 and gridMET totals in 2016 were attributable to changes in input data. Increases in decadal precipitation for TerraClimate and gridMET were 23% and 28% larger than those of the reference gauges (Fig. 6 and S5). The 2011 TerraClimate shift reflected the substitution of JRA-55 anomalies following a sharp gauge decline (Abatzoglou et al., 2018), while the 2016 gridMET inhomogeneity coincided with a reprocessed precipitation forcing that incorporated late-reporting gauges (Xia et al., 2016).





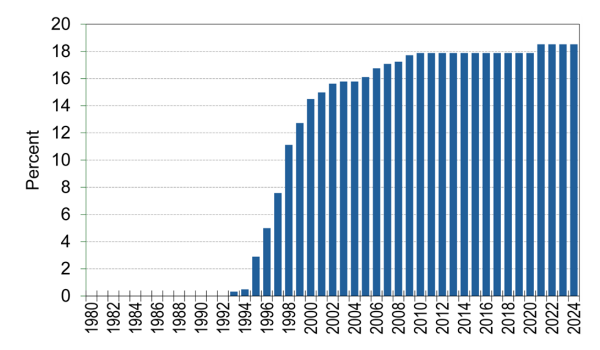


Figure 9. Percent coverage of the southeastern United States over time by Automated Surface Observing Systems (ASOS) gauges.

5.2 Optimal Dataset for Multi-Decadal Precipitation Analyses

Combining Daymet and nClimGrid results in a more homogeneous and reliable dataset for multi-decadal precipitation analyses in the Southeast. Among the 15 monthly and 15 daily datasets evaluated using annual precipitation totals, this combination yields the fourth-smallest cumulative sum of absolute residuals (Fig. 5) and has no significant inhomogeneities (Fig. 6). The precipitation trend (29 mm dec⁻¹) of Daymet–nClimGrid closely matched the reference trend (30 mm dec⁻¹), and no other product reproduced the reference trend as accurately (Fig. 8). Season-specific analyses also revealed no evidence of inhomogeneities and exhibited trends nearly identical to those of the reference series (Fig. 10), further supporting the reliability of the dataset for multi-decadal assessment. Although using this dataset reduces the spatial resolution inherent to Daymet, the resulting gain in temporal homogeneity makes the Daymet–nClimGrid product the most robust dataset for regional, multi-decadal precipitation assessments.

6 Conclusion

Gridded precipitation datasets commonly used for hydroclimatic analyses exhibit widespread temporal inhomogeneities that can distort long-term trend assessments. Evaluation of five high-resolution products and their combinations for the southeastern United States during 1980–2024 revealed significant inhomogeneities in about 80% of the series, primarily between 2002 and 2018, linked to changes in gauge networks and data processing. Wetting biases in Daymet and PRISM reflected the expansion of CoCoRaHS and decline of COOP gauges, whereas a drying bias in nClimGrid arose from increased reliance on ASOS tipping-bucket gauges. Step changes in TerraClimate and gridMET corresponded to shifts in input data and processing. These inhomogeneities produced precipitation trends ranging from 19 to 48 mm dec⁻¹, compared with a non-significant reference trend of 30 mm dec⁻¹. Combining Daymet and nClimGrid removed detectable inhomogeneities and reproduced the reference trend, providing the most temporally stable dataset for multi-decadal analyses. Overall, the results underscore the need to assess and, where possible, improve the temporal stability of gridded precipitation datasets used in long-term hydroclimatic analyses.





247 248

249

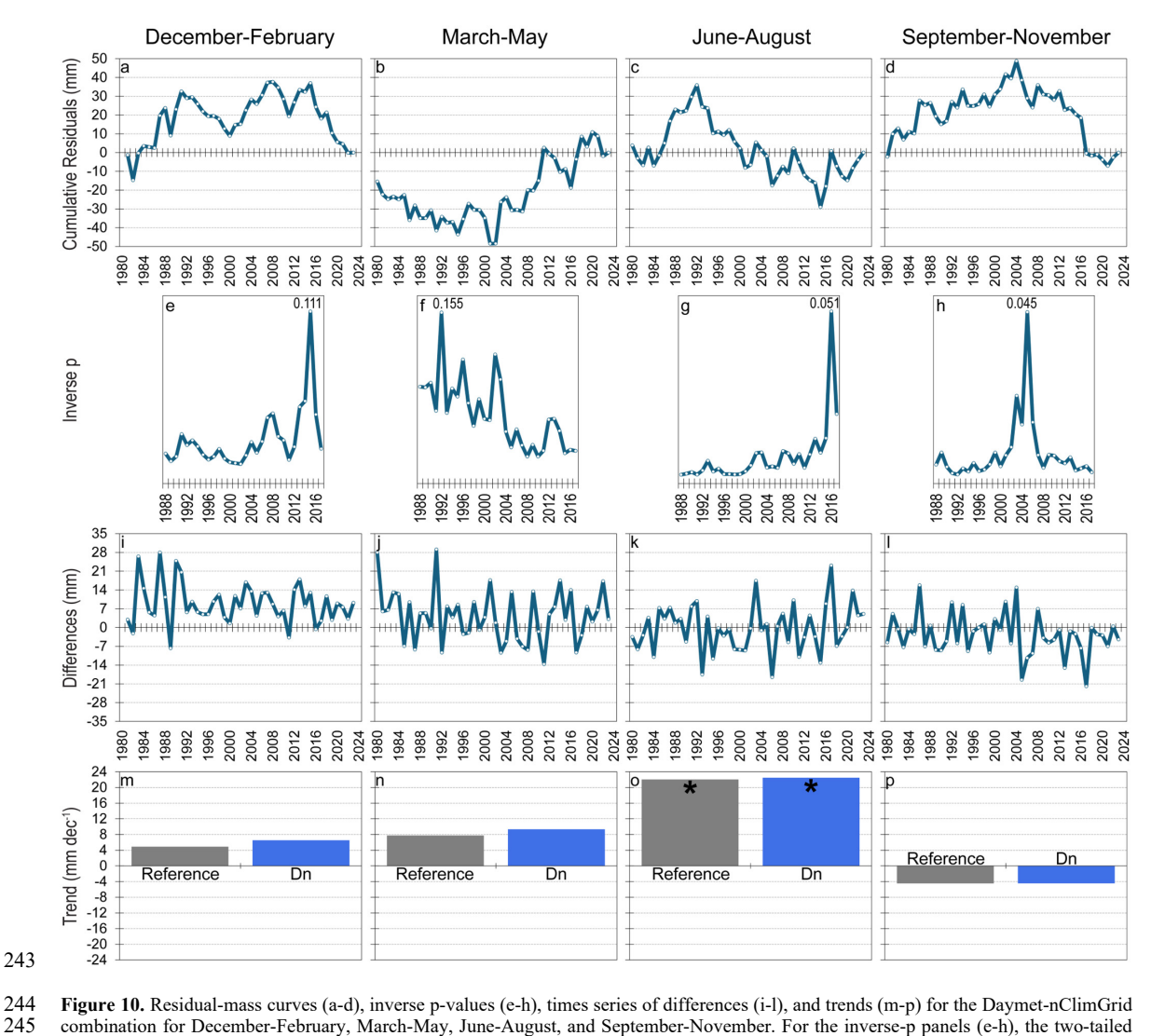


Figure 10. Residual-mass curves (a-d), inverse p-values (e-h), times series of differences (i-l), and trends (m-p) for the Daymet-nClimGrid combination for December-February, March-May, June-August, and September-November. For the inverse-p panels (e-h), the two-tailed p-values are from Mann-Whitney U tests that compared differences from the reference time series before and after each of the years shown (i.e., 1988-2018). The values in the difference panels (i-l) are precipitation totals from the products minus totals from the reference gauges. For the trends panels (m-p), the reference trend pertains to the reference time series and asterisks denote significant ($\alpha = 0.01$, one-tailed) trends over 1980-2023.





- 250 Data availability. Data used in this paper are available at https://data.mendeley.com/datasets/37bm8hvpmk/1.
- 251 Competing interests. The author does not have any competing interests.

252 References

- Abatzoglou, J. T.: Development of gridded surface meteorological data for ecological applications and modelling, Int. J. Climatol., 33, 121–131, https://doi.org/10.1002/joc.3413, 2013.
- Abatzoglou, J. T., Dobrowski, S. Z., Parks, S. A., and Hegewisch, K. C.: TerraClimate, a high-resolution global dataset of
 monthly climate and climatic water balance from 1958–2015, Sci. Data, 5, 170191,
 https://doi.org/10.1038/sdata.2017.191, 2018.
- Buishand, T. A.: Tests for detecting a shift in the mean of hydrological time series, J. Hydrol., 73, 51–69,
 https://doi.org/10.1016/0022-1694(84)90032-5, 1984.
- CoCoRaHS (Community Collaborative Rain, Hail & Snow Network): Why CoCoRaHS requires manual measurements,
 CoCoRaHS Headquarters, Fort Collins, CO, available at:
- 262 https://media.cocorahs.org/docs/Why%20CoCoRaHS%20requires%20manual%20measurements.pdf, 2019.
- Daly, C., Doggett, M. K., Smith, J. I., Olson, K. V., Halbleib, M. D., Dimcovic, Z., Keon, D., Loiselle, R. A., Steinberg, B.,
 Ryan, A. D., Pancake, C. M., and Kaspar, E. M.: Challenges in observation-based mapping of daily precipitation across
 the conterminous United States, J. Atmos. Ocean. Technol., 38, 1979–1992, https://doi.org/10.1175/JTECH-D-21-0054.1, 2021.
- De La Fraga, P., Del-Toro-Guerrero, F. J., Vivoni, E. R., Cavazos, T., and Kretzschmar, T.: Evaluation of gridded
 precipitation datasets in mountainous terrains of Northwestern Mexico, J. Hydrol.: Reg. Stud., 56, 102019,
 https://doi.org/10.1016/j.ejrh.2024.102019, 2024.
- Döll, P., Douville, H., Güntner, A., Müller Schmied, H., and Wada, Y.: Modelling freshwater resources at the global scale: challenges and prospects, Surv. Geophys., 37, 195–221, https://doi.org/10.1007/s10712-015-9343-1, 2016.
- Durre, I., Arguez, A., Schreck, C. J., Squires, M. F., and Vose, R. S.: Daily high-resolution temperature and precipitation
 fields for the contiguous United States from 1951 to present, J. Atmos. Ocean. Technol., 39, 1837–1855,
 https://doi.org/10.1175/JTECH-D-22-0024.1, 2022.
- Easterling, D. R. and Peterson, T. C.: A new method for detecting undocumented discontinuities in climatological time series, Int. J. Climatol., 15, 369–377, https://doi.org/10.1002/joc.3370150403, 1995.
- Ferencz, S. B., Sun, N., Turner, S. W. D., Smith, B. A., and Rice, J. S.: Multisectoral analysis of drought impacts and management responses to the 2008–2015 record drought in the Colorado Basin, Texas, Nat. Hazards Earth Syst. Sci., 24, 1871–1896, https://doi.org/10.5194/nhess-24-1871-2024, 2024.
- Ferguson, C. R. and Mocko, D. M.: Diagnosing an artificial trend in NLDAS-2 afternoon precipitation, J. Hydrometeorol., 18, 1051–1070, https://doi.org/10.1175/JHM-D-16-0251.1, 2017.
- Goble, P. E., Doesken, N. J., Durre, I., Schumacher, R. S., Stewart, A., and Turner, J.: Who received the most rain today?:
 An analysis of daily precipitation extremes in the contiguous United States using CoCoRaHS and COOP reports, Bull.
 Am. Meteorol. Soc., 101, E710–E719, https://doi.org/10.1175/BAMS-D-18-0310.1, 2019.
- Guentchev, G., Barsugli, J. J., and Eischeid, J.: Homogeneity of gridded precipitation datasets for the Colorado River Basin,
 J. Appl. Meteorol. Climatol., 49, 2404–2415, https://doi.org/10.1175/2010JAMC2484.1, 2010.
- Helsel, D. R., and Hirsch, R. M.: Statistical methods in water resources, Techniques of Water-Resources Investigations, Book 4, Chapter A3, U.S. Geological Survey, available at: https://pubs.usgs.gov/twri/twri4a3/, 2002.
- Henn, B., Newman, A. J., Livneh, B., Daly, C., and Lundquist, J. D.: An assessment of differences in gridded precipitation datasets in complex terrain, J. Hydrol., 556, 1205–1219, https://doi.org/10.1016/j.jhydrol.2017.03.008, 2018.
- Kidd, C., Becker, A., Huffman, G. J., Muller, C. L., Joe, P., Skofronick-Jackson, G., and Kirschbaum, D. B.: So, How much of the Earth's surface is covered by rain gauges?, Bull. Am. Meteorol. Soc., 98, 69–78, https://doi.org/10.1175/BAMS-D-14-00283.1, 2017.





- Kunkel, K. E., Stevens, L. E., Stevens, S. E., Sun, L., Janssen, E., Wuebbles, D., Konrad, C. E. II, Fuhrman, C. M., Keim, B.
- 295 D., Kruk, M. C., Billot, A., Needham, H., Shafer, M., and Dobson, J. G.: Regional climate trends and scenarios for the
- 296 U.S. National Climate Assessment. Part 2: Climate of the Southeast U.S., NOAA Tech. Rep. NESDIS 142-2, National 297 Oceanic and Atmospheric Administration, Washington, DC, 2013.
- 298 Labosier, C. and Quiring, S.: Hydroclimatology of the Southeastern USA, Clim. Res., 57, 157–171, 299 https://doi.org/10.3354/cr01166, 2013.
- 300 Laiti, L., Mallucci, S., Piccolroaz, S., Bellin, A., Zardi, D., Fiori, A., Nikulin, G., and Majone, B.: Testing the hydrological 301 coherence of high-resolution gridded precipitation and temperature data sets, Water Resour. Res., 54, 1999-2016, 302 https://doi.org/10.1002/2017WR021633, 2018.
- 303 Livneh, B., Bohn, T. J., Pierce, D. W., Munoz-Arriola, F., Nijssen, B., Vose, R., Cayan, D. R., and Brekke, L.: A spatially 304 comprehensive, hydrometeorological data set for Mexico, the U.S., and Southern Canada 1950-2013, Sci. Data, 2, 305 150042, https://doi.org/10.1038/sdata.2015.42, 2015.
- 306 Mankin, K. R., Mehan, S., Green, T. R., and Barnard, D. M.: Review of gridded climate products and their use in 307 hydrological analyses reveals overlaps, gaps, and the need for a more objective approach to selecting model forcing datasets, Hydrol. Earth Syst. Sci., 29, 85–108, https://doi.org/10.5194/hess-29-85-2025, 2025. 308
- 309 McAfee, S., Guentchev, G., and Eischeid, J.: Reconciling precipitation trends in Alaska: 2. Gridded data analyses, J. Geophys. Res.: Atmos., 119, https://doi.org/10.1002/2014JD022461, 2014. 310
- Michelon, A., Benoit, L., Beria, H., Ceperley, N., and Schaefli, B.: Benefits from high-density rain gauge observations for 311 312 hydrological response analysis in a small alpine catchment, Hydrol. Earth Syst. Sci., 25, 2301-2325, 313 https://doi.org/10.5194/hess-25-2301-2021, 2021.
- 314 Mizukami, N. and Smith, M. B.: Analysis of inconsistencies in multi-year gridded quantitative precipitation estimate over complex terrain and its impact on hydrologic modeling, J. Hydrol., 428-429, 129-141, 315 316 https://doi.org/10.1016/j.jhydrol.2012.01.030, 2012.
- Muche, M. E., Sinnathamby, S., Parmar, R., Knightes, C. D., Johnston, J. M., Wolfe, K., Purucker, S. T., Cyterski, M. J., and 317 318 Smith, D.: Comparison and evaluation of gridded precipitation datasets in a Kansas agricultural watershed using SWAT, 319 J. Am. Water Resour. Assoc., 56, 486–506, https://doi.org/10.1111/1752-1688.12819, 2020.
- 320 National Research Council: Future of the National Weather Service Cooperative Observer Network, The National 321 Academies Press, Washington, DC, 1998.
- 322 National Research Council: The National Weather Service modernization and associated restructuring: A retrospective 323 assessment, The National Academies Press, Washington, DC, 2012.
- 324 New, M., Todd, M., Hulme, M., and Jones, P.: Precipitation measurements and trends in the twentieth century, Intl Journal 325 of Climatology, 21, 1889–1922, https://doi.org/10.1002/joc.680, 2001.
- 326 Newman, A. J., Clark, M. P., Sampson, K., Wood, A., Hay, L. E., Bock, A., Viger, R. J., Blodgett, D., Brekke, L., Arnold, J. 327 R., Hopson, T., and Duan, Q.: Development of a large-sample watershed-scale hydrometeorological data set for the
- 328 contiguous USA: data set characteristics and assessment of regional variability in hydrologic model performance, Hydrol.
- 329 Earth Syst. Sci., 19, 209–223, https://doi.org/10.5194/hess-19-209-2015, 2015.
- Peterson, T. C., Easterling, D. R., Karl, T. R., Groisman, P., Nicholls, N., Plummer, N., Torok, S., Auer, I., Boehm, R., 330
- 331 Gullett, D., Vincent, L., Heino, R., Tuomenvirta, H., Mestre, O., Szentimrey, T., Salinger, J., Førland, E. J., Hanssen-
- 332 Bauer, I., Alexandersson, H., Jones, P., and Parker, D.: Homogeneity adjustments of in situ atmospheric climate data: a 333 review, Int. J. Climatol., 18, 1493-1517, https://doi.org/10.1002/(SICI)1097-0088(19981115)18:13<1493::AID-
- 334 JOC329>3.0.CO;2-T, 1998.
- 335 Searcy, J. K., and Hardison, C. H.: Double-mass curves, in: Manual of Hydrology: Part 1, General Surface-Water 336 Techniques, U.S. Geological Survey Water-Supply Paper 1541-B, 31-66, 1960.
- Shuai, P., Chen, X., Mital, U., Coon, E. T., and Dwivedi, D.: The effects of spatial and temporal resolution of gridded 337 338 meteorological forcing on watershed hydrological responses, Hydrol. Earth Syst. Sci., 26, 2245-2276,
- 339 https://doi.org/10.5194/hess-26-2245-2022, 2022.
- 340 Tang, G., Behrangi, A., Long, D., Li, C., and Hong, Y.: Accounting for spatiotemporal errors of gauges: a critical step to 341 evaluate gridded precipitation products, J. Hydrol., 559, 294–306, https://doi.org/10.1016/j.jhydrol.2018.02.057, 2018.





- 342 Tang, G., Clark, M. P., Knoben, W. J. M., Liu, H., Gharari, S., Arnal, L., Wood, A. W., Newman, A. J., Freer, J., and
- Papalexiou, S. M.: Uncertainty hotspots in global hydrologic modeling: the impact of precipitation and temperature
- 344 forcings, Bull. Am. Meteorol. Soc., 106, E146–E166, https://doi.org/10.1175/BAMS-D-24-0007.1, 2025.
- Thornton, P. E., Shrestha, R., Thornton, M., Kao, S.-C., Wei, Y., and Wilson, B. E.: Gridded daily weather data for North
- America with comprehensive uncertainty quantification, Sci. Data, 8, 190, https://doi.org/10.1038/s41597-021-00973-0, 2021.
- 348 Vose, R. S., Applequist, S., Squires, M., Durre, I., Menne, M. J., Williams, C. N., Fenimore, C., Gleason, K., and Arndt, D.:
- Improved historical temperature and precipitation time series for U.S. climate divisions, J. Appl. Meteorol. Climatol., 53, 1232–1251, https://doi.org/10.1175/JAMC-D-13-0248.1, 2014.
- 351 Wade, C. G.: A multisensor approach to detecting drizzle on ASOS*, J. Atmos. Oceanic Technol., 20, 820-832,
- 352 https://doi.org/10.1175/1520-0426(2003)020<0820:AMATDD>2.0.CO;2, 2003.
- Wang, F. and Tian, D.: Hourly Evaluation of eight gridded precipitation datasets over the contiguous United States:
- intercomparison of satellite, radar, reanalysis, and merged products, J. Hydrometeorol., 26, 1717–1733,
- 355 https://doi.org/10.1175/JHM-D-25-0063.1, 2025.
- Xia, Y., Mocko, D., and Rodell, M.: An upgrade from current OPS NLDAS-2 system, in: Conference Presentation, NASA
 Goddard Space Flight Center, 7 July 2016.
- Yang, D., Yang, Y., and Xia, J.: Hydrological cycle and water resources in a changing world: a review, Geogr. Sustain., 2,
 115–122, https://doi.org/10.1016/j.geosus.2021.05.003, 2021.
- Yue, S. and Wang, C. Y.: Power of the Mann-Whitney test for detecting a shift in median or mean of hydro-meteorological data, Stoch. Environ. Res. Risk Assess., 16, 307–323, https://doi.org/10.1007/s00477-002-0101-9, 2002.
- Zandler, H., Haag, I., and Samimi, C.: Evaluation needs and temporal performance differences of gridded precipitation products in peripheral mountain regions, Sci. Rep., 9, 15118, https://doi.org/10.1038/s41598-019-51666-z, 2019.